ISSN: 0256-307X

中国物理快报

Chinese Physics Letters

Volume 35 Number 7 July 2018

A Series Journal of the Chinese Physical Society
Distributed by IOP Publishing

Online: http://iopscience.iop.org/0256-307X
http://cpl.iphy.ac.cn

CHINESE PHYSICAL SOCIETY
IOP Publishing

CHIN. PHYS. LETT. Vol. 35, No. 7 (2018) 070301

Period-Doubled Bloch States in a Bose–Einstein Condensate *

Bao-Guo Yang(杨保国)[1], Peng-Ju Tang(唐鹏举)[1], Xin-Xin Guo(郭新新)[1], Xu-Zong Chen(陈徐宗)[1], Biao Wu(吴飙)[2**], Xiao-Ji Zhou(周小计)[1**]

[1]*School of Electronics Engineering and Computer Science, Peking University, Beijing 100871*
[2]*International Center for Quantum Materials, School of Physics, Peking University, Beijing 100871*

(Received 2 May 2018)

We study systematically the period-doubled Bloch states for a weakly interacting Bose–Einstein condensate in a one-dimensional optical lattice. This kind of state is of form $\psi_k = e^{ikx}\phi_k(x)$, where $\phi_k(x)$ is of a period twice the optical lattice constant. Our numerical results show how these nonlinear period-doubled states grow out of linear period-doubled states at a quarter away from the Brillouin zone center as the repulsive interatomic interaction increases. This is corroborated by our analytical results. We find that all nonlinear period-doubled Bloch states have both Landau instability and dynamical instability.

PACS: 03.75.Lm, 67.85.Hj, 67.85.Bc, 67.85.De DOI: 10.1088/0256-307X/35/7/070301

A Bose–Einstein condensate (BEC) in an optical lattice (OL) has been explored theoretically and experimentally for its rich physics,[1] such as quantum phase transition,[2–5] unconventional superfluidity,[6] and various nonlinear effects.[7–20] In the mean-field theory, a BEC in an OL becomes a nonlinear periodic system, which exhibits many features that cannot be found in a linear periodic system. For example, the nonlinear periodic system can have loop structures in its Bloch band.[10–17] Such a nonlinear system can have a type of solution called gap solitons, which are localized in space and whose chemical potential lies in the linear band gap.[18–20] These gap solitons can never exist in a linear periodic system. There is another type of solutions, which are Bloch-like states but their periodic parts have a period that is twice the lattice constant.[21] These period-doubled states are closely related to the period-doubling phenomenon that has been observed experimentally.[22]

In this Letter, we investigate these period-doubled states systematically for a BEC in a one-dimensional OL. It is found that these states can be Bloch-like and the corresponding chemical potentials form Bloch-like bands. Our numerical results show that when the repulsive interatomic interaction increases from zero, the period-doubled band begins to emerge around the quasi-momentum that is a quarter away from the Brillouin zone center (see Fig. 2). As the interaction further increases, the period-doubled band extends to the whole Brillouin zone. We have also analyzed the situation when the interaction is very small. Our analytical results are very consistent with our numerical results. Computing their Bogoliubov spectrums, we further find that all nonlinear period-doubled states have Landau instability and dynamical instability.

We consider a weakly-interacting BEC in a one-dimensional OL. In the mean-field regime, this system can be well described by the following Gross–Pitaevskii equation (GPE)[23]

$$i\hbar\frac{\partial\Phi(\tilde{\boldsymbol{r}},\tilde{t})}{\partial\tilde{t}} = -\frac{\hbar^2}{2m}\nabla^2\Phi(\tilde{\boldsymbol{r}},\tilde{t}) + \tilde{V}(\tilde{\mathbf{r}})\Phi(\tilde{\boldsymbol{r}},\tilde{t}) + \frac{4\pi\hbar^2 a_{\rm s}}{m}|\Phi(\tilde{\boldsymbol{r}},\tilde{t})|^2\Phi(\tilde{\boldsymbol{r}},\tilde{t}), \quad (1)$$

where $a_{\rm s}$ is the s-wave scattering length, and m is the atomic mass. We consider a cigar-shaped condensate,[24,25] thus we can focus only on the lattice direction and ignore the other directions. Mathematically, we can write the matter wave function as

$$\Phi(\tilde{\boldsymbol{r}},\tilde{t}) = \varphi(\tilde{x},\tilde{t})\varphi_0(\tilde{y},\tilde{z})e^{-i(E_y+E_z)\tilde{t}/\hbar}, \quad (2)$$

where φ_0 is the wave function in the transverse direction of the BEC with the corresponding energy $E_y + E_z$, which can be approximated by the Gaussian function. Thus Eq. (1) can be reduced to a one-dimensional form

$$i\hbar\frac{\partial\varphi(\tilde{x},\tilde{t})}{\partial\tilde{t}} = -\frac{\hbar^2}{2m}\frac{\partial^2\varphi(\tilde{x},\tilde{t})}{\partial\tilde{x}^2} + V(\tilde{x})\varphi(\tilde{x},\tilde{t}) + \frac{4\pi\hbar^2 a_{\rm s}}{mA}|\varphi(\tilde{x},\tilde{t})|^2\varphi(\tilde{x},\tilde{t}), \quad (3)$$

where $A = 2/|\varphi_0(0,0)|^2$ is the effective cross sectional area of the condensate. In the longitudinal direction, we do not consider the harmonic trap, and the OL potential is given by

$$V(\tilde{x}) = V_0\cos^2(k_{\rm L}\tilde{x}) = \frac{V_0}{2}\cos(2k_{\rm L}\tilde{x}) + \frac{V_0}{2}, \quad (4)$$

where $k_{\rm L} = 2\pi/\lambda$ with λ being the wavelength of the laser, and V_0 is the lattice depth. After neglecting the

*Supported by the National Key Research and Development Program of China under Grant Nos 2016YFA0301501 and 2017YFA0303302, and the National Natural Science Foundation of China under Grants Nos 11334001, 61727819, 61475007 and 91736208.

**Corresponding author. Email: wubiao@pku.edu.cn; xjzhou@pku.edu.cn

constant potential $V_0/2$, the dimensionless GPE is

$$i\frac{\partial\Psi(x,t)}{\partial t} = -\frac{1}{2}\frac{\partial^2\Psi(x,t)}{\partial x^2} + \frac{v}{2}\cos(x)\Psi(x,t) + \frac{c}{8}|\Psi(x,t)|^2\Psi(x,t), \quad (5)$$

where $\Psi(x,t) = \sqrt{\pi/(N_0 k_{\rm L})}\varphi(\tilde{x},\tilde{t})$, with N_0 being the total number of atoms, x is in units of $1/2k_{\rm L}$, t is in units of $m/4\hbar k_{\rm L}^2$, and the potential well depth v is in units of $8E_{\rm r}$ with $E_{\rm r} = \hbar^2 k_{\rm L}^2/2m$ the recoil energy. The interaction constant $c = 8\pi a_{\rm s} n_0/k_{\rm L}^2$ with $n_0 = N_0 k_{\rm L}/(\pi A)$ the averaged density of BEC. Substituting $\Psi(x,t) = \psi(x)e^{-i\mu t}$ into Eq. (5), we obtain the time-independent GPE

$$-\frac{1}{2}\frac{d^2\psi(x)}{dx^2} + \frac{v}{2}\cos(x)\psi(x) + \frac{c}{8}|\psi(x)|^2\psi(x) = \mu\psi(x), \quad (6)$$

where μ is the nonlinear eigenvalue, and $\psi(x)$ satisfies the following normalization condition

$$\int_{-l\pi}^{l\pi}|\psi(x)|^2 dx = 2l\pi, \quad (7)$$

with $l = 1$ for single-period solutions and $l = 2$ for period-doubled solutions.

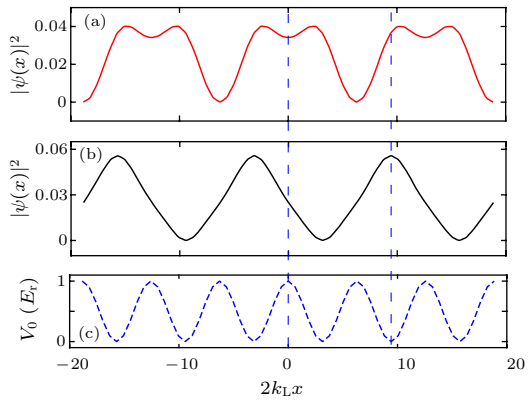

Fig. 1. (Color online) Two types of period-doubled Bloch states. (a) Type I, whose peaks are around the crests of the lattice potential, and (b) type II, whose peaks are around the troughs. The lattice potential is shown in (c). Quasi-momentum $k = 0.25$, OL depth $V_0 = 1E_{\rm r}$, and $c = 0.5$.

When $c = 0$, the solutions to Eq. (6) are usual Bloch waves, which can be expressed as

$$\psi_k^0(x) = e^{ikx}u_k(x) = e^{ikx}u_k(x+2\pi), \quad (8)$$

where $\hbar k$ is the quasi-momentum. When $c \neq 0$, in addition to these usual Bloch waves, there exist solutions in the form

$$\psi_k(x) = e^{ikx}\phi_k(x) = e^{ikx}\phi_k(x+4\pi). \quad (9)$$

We call these solutions period-doubled Bloch waves. Substituting Eq. (9) into Eq. (6), we have

$$-\frac{1}{2}\Big(\frac{d}{dx}+ik\Big)^2\phi_k + \frac{v}{2}\cos(x)\phi_k + \frac{c}{8}|\phi_k|^2\phi_k = \mu(k)\phi_k. \quad (10)$$

These period-doubled Bloch states $\phi_k(x)$ can be expanded in the following Fourier series

$$\phi_k(x) = \sum_{n=-N}^{N} a_n e^{i\frac{n}{2}x}, \quad (11)$$

where N is the cutoff. Substituting Eq. (11) into Eq. (10), we have

$$\frac{1}{2}\Big(\frac{n}{2}+k\Big)^2 a_n + \frac{v}{4}(a_{n-2}+a_{n+2}) + \frac{c}{8}\sum_{n_1=-N}^{N}\sum_{n_2=-N}^{N} a_{n_1}^* a_{n_2} a_{n-n_2+n_1} = \mu a_n. \quad (12)$$

Numerically solving the above equations for a_n and μ together with the normalization condition $\sum_{n=-N}^{N}|a_n|^2 = 1$, we can find both the single-period and period-doubled solutions. The results are plotted in Figs. 1 and 2 with OL depth $V_0 = 1E_{\rm r}$. For the period-doubled Bloch waves, their Brillouin zone is only half the Brillouin zone of the usual single-period Bloch waves. Therefore, to compare between the usual Bloch states and period-doubled solutions, we have folded up the first Brillouin zone for the usual Bloch states in Fig. 2.

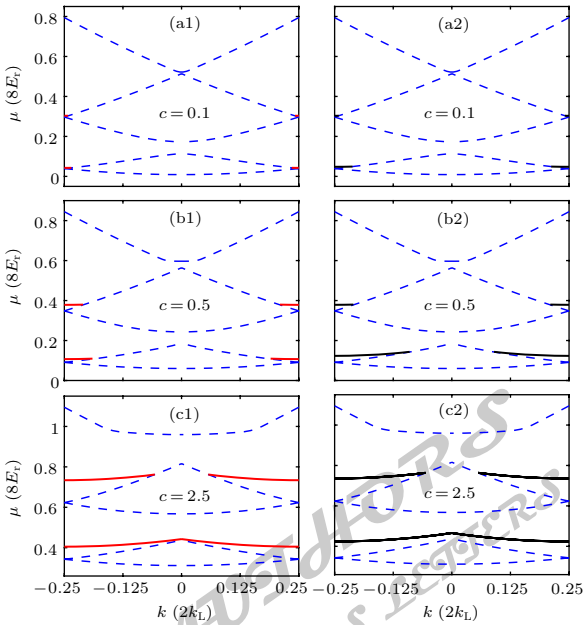

Fig. 2. (Color online) Energy bands for period-doubled Bloch states: type I on the left (red solid curves) and type II on the right (black solid curves). Energy bands for single-period (blue dashed curves) are plotted for comparison. Here [(a1), (a2)] $c = 0.1$; [(b1), (b2)] $c = 0.5$; [(c1), (c2)] $c = 2.5$, and $V_0 = 1E_{\rm r}$.

There are two types of period-doubled Bloch states as shown in Fig. 1. For type-I states, mathematically their coefficients a_n are all real; physically, their peaks are around the crests of the lattice potential

(see Fig. 1(a)). For type Ⅱ, mathematically their coefficients a_n's are real for even n and pure imaginary for odd n; physically, their peaks are around the troughs of the lattice potential (see Fig. 1(b)).

Similar to the usual Bloch waves, the period-doubled Bloch states can also form energy bands. These energy bands in terms of chemical potential $\mu(k)$ are plotted in Fig. 2, where they are compared with the usual Bloch bands. It is clear from Fig. 2 that the period-doubled Bloch bands start at $k = 1/4$, where the fold-up single-period Bloch bands are degenerate. As the interaction becomes stronger, that is, c increases, the period-doubled bands extend further toward the Brillouin zone center. Around $c = 2.5$, the lowest period-doubled bands for both types I and Ⅱ are extended over the full Brillouin zone. We have plotted these period-doubled bands for different c together in Fig. 3, where one can see more clearly how the bands grow as c increases. Or, one can view it reversely and see how these period-doubled Bloch bands disappear when the interaction c is reduced to zero. These numerical results strongly suggest that the period-doubled Bloch states are grown out of some 'seeds' in the usual single-period Bloch states. In the following we take a closer look analytically.

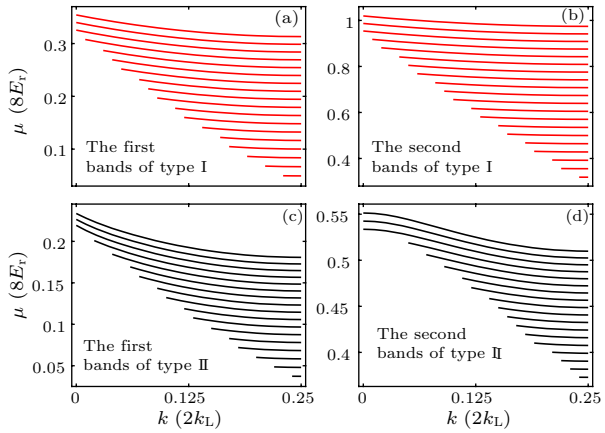

Fig. 3. (Color online) Period-doubled energy bands for different atomic interactions c. The upper two panels (a) and (b) are for type-I period-doubled Bloch states; the lower two panels (c) and (d) are for type-Ⅱ states. (a) From bottom to top, the first bands of type I are for c ranging from 0.1 to 1.8 with a step size of 0.1; $V_0 = 0.1E_r$. (b) From bottom to top, the second bands of type I are for c ranging from 0.2 to 4 with a step size of 0.2; $V_0 = 0.1E_r$. (c) From bottom to top, the first bands of type I are for c ranging from 0.05 to 0.85 with a step size of 0.05; $V_0 = 1E_r$. (d) From bottom to top, the second bands of type Ⅱ are for c ranging from 0.04 to 0.55 with a step size of 0.03; $V_0 = 10E_r$.

Considering the linear case $c = 0$ and the lowest band, with the usual Bloch waves, we can construct period-doubled states as follows:

$$\begin{aligned}\varphi_k^0(x) &= c_1\psi_k^0(x) + c_2\psi_{k-\frac{1}{2}}^0(x)\\ &= e^{ikx}[c_1 u_k(x) + c_2 e^{-ix/2}u_{k-\frac{1}{2}}(x)],\end{aligned} \quad (13)$$

where c_1 and c_2 are complex and satisfy $|c_1|^2+|c_2|^2 = 1$. These period-doubled states $\varphi_k^0(x)$ are solutions to Eq. (6) with $c = 0$ only when $k = 1/4$. Our numerical results show that as c decreases to zero the nonlinear period-doubled Bloch states in the lowest bands shown in Figs. 1–3 are reduced to $\varphi_{\frac{1}{4}}^0(x)$ with specified c_1 and c_2. To specify c_1 and c_2, we need to fix the phases of the usual Bloch states $\phi_k^0(x)$. In Eq. (11), our phase convention is taken in such a way that the largest coefficient $a_{\rm m}$ is real and positive. With this phase convention, according to our numerical calculation, type I is connected to

$$\varphi_{1/4}^0(x) = \frac{1}{\sqrt{2}}[\psi_{1/4}^0(x) \pm \psi_{-1/4}^0(x)], \quad (14)$$

and type Ⅱ is to

$$\varphi_{1/4}^0(x) = \frac{1}{\sqrt{2}}[\psi_{1/4}^0(x) \pm i\psi_{-1/4}^0(x)]. \quad (15)$$

The results are similar for the second or higher bands of period-doubled Bloch states.

The above numerical results have given us clear guidance on how to obtain some analytical results, in particular, when c is small. When c increases slightly from zero, we observe that two things will happen. (i) The period-doubled states $\varphi_{1/4}^0(x)$ will persist with slightly modified form. (ii) New period-doubled states slightly away from $k = 1/4$ will emerge. When $k \neq 1/4$ and $c = 0$, the states $\varphi_k^0(x)$ in Eq. (13) are not solutions to Eq. (6) due to the fact that ψ_k^0 and $\psi_{k-\frac{1}{2}}^0$ have different eigen energies. When c is not zero, the interaction energy may bridge this energy gap and render $\varphi_k^0(x)$ as the solutions to Eq. (6).

Based on observation (i), we expect the nonlinear period-doubled Bloch state to have the following form

$$\begin{aligned}\psi_{\frac{1}{4}}(x) \approx \sqrt{\frac{1}{2}-\delta^2}[\psi_{1,\frac{1}{4}}^0(x) \pm e^{i\theta_0}\psi_{1,-\frac{1}{4}}^0(x)]\\ + \delta[\psi_{2,\frac{1}{4}}^0(x) \pm e^{i\theta_0}\psi_{2,-\frac{1}{4}}^0(x)],\end{aligned} \quad (16)$$

where $\theta_0 = 0$ for type I and $\theta_0 = \pi/2$ for type Ⅱ. The integers in the subscript of ψ^0 are band indices as the states in the second linear Bloch band are involved due to interaction. Here δ is small and has the same order of magnitude of c. Substituting the above $\psi_{1/4}(x)$ into Eq. (6), and keeping to the first-order correction, we obtain

$$\mu_{\frac{1}{4}} = \mu_{1,\frac{1}{4}}^0 + \frac{c}{64\pi}\int_{-\pi}^{\pi}|\psi_{1,\frac{1}{4}}^0 \pm e^{i\theta_0}\psi_{1,-\frac{1}{4}}^0|^4 {\rm d}x. \quad (17)$$

This result is plotted in Fig. 4(a) as a function of c with the red dashed curve for type I and the black solid curve for type Ⅱ. The corresponding numerical results are shown with blue crosses and circles, respectively. It is clear from Fig. 4(a) that our above approximation is reasonably good.

For observation (ii), we consider period-doubled states with k less than but close to 1/4. In this case

we only need to consider the lowest linear band and approximate the nonlinear period-doubled states as

$$\psi_k(x) = \sqrt{\frac{1}{2}+\delta}\psi_k^0(x) \pm e^{i\theta_0}\sqrt{\frac{1}{2}-\delta}\psi_{k-\frac{1}{2}}^0(x). \quad (18)$$

Substituting Eq. (18) into Eq. (6), we find that the chemical potential can be approximated as

$$\mu_k = \frac{\mu_k^0+\mu_{k-\frac{1}{2}}^0}{2} + \frac{c}{64\pi}\int_{-\pi}^{\pi}|\psi_k^0 \pm e^{i\theta_0}\psi_{k-\frac{1}{2}}^0|^4 dx. \quad (19)$$

This analytical result is compared with the corresponding numerical ones in Fig. 4(b), where the red curve is for $\theta_0 = 0$ and the black one is for $\theta_0 = \pi/2$. The corresponding numerical results are marked with crosses and circles. We can see that they are very consistent with each other.

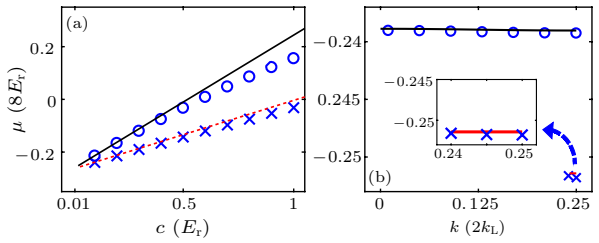

Fig. 4. (Color online) Comparison between analytical results and numerical results for chemical potentials of period-doubled Bloch states. The analytical results are given by red dashed curves for type I and black solid curves for type Ⅱ, and the numerical ones are given by blue circles and crosses, respectively. (a) Chemical potentials at $k = 1/4$ as a function of the interaction strength c. (b) Period-doubled energy bands for $c = 0.05$. As the band for type I is very narrow, it is zoomed up in the inset. Here $V_0 = 10E_r$.

The stability of the usual Bloch states has been studied both theoretically and experimentally.[11,26–32] It is found that many of the usual Bloch states near the Brillouin zone edge $\pm k_L$ are unstable, suffering both Landau instability and dynamical instability. It is worthwhile and also necessary to examine the stability of these period-doubled Bloch states.

As the details of how to examine Landau instability and dynamical instability have been spelled out,[14] we just briefly summarize the procedure. To study Landau instability, we need to compute the eigenvalues of the following matrix

$$M_k(q) = \begin{pmatrix} \mathscr{L}(k+q) & \frac{c}{8}\phi_k^2 \\ \frac{c}{8}\phi_k^{*2} & \mathscr{L}(-k+q) \end{pmatrix}, \quad (20)$$

where q is the perturbation Bloch wave number, and

$$\mathscr{L}(k) = -\frac{1}{2}\left(\frac{\partial}{\partial x}+ik\right)^2 + \frac{v}{2}\cos(x) + \frac{c}{4}|\phi_k(x)|^2 - \mu. \quad (21)$$

Diagonalizing the matrix $M_k(q)$, we can obtain the eigenvalues. If $M_k(q)$ is positive definite for all $-0.25 \le q \le 0.25$ for period-doubled solutions, the solution $\phi_k(x)$ is a local minimum and has no Landau instability. If $M_k(q)$ has negative eigenvalues for some q, the Bloch wave is a saddle point and suffers Landau instability.

For dynamical instability, we need to diagonalize another matrix $\sigma_z M_k(q)$, where

$$\sigma_z = \begin{pmatrix} I & 0 \\ 0 & -I \end{pmatrix}. \quad (22)$$

If all eigenvalues of $\sigma_z M_k(q)$ are real for all $-0.25 \le q \le 0.25$ for period-doubled solutions, the period-doubled state is dynamically stable. If there are complex eigenvalues, the initial small disturbance can grow exponentially in time, and the state is dynamically unstable. We denote the maximum values among the imaginary part of eigenvalues of matrix $\sigma_z M_k(q)$ as M_D.

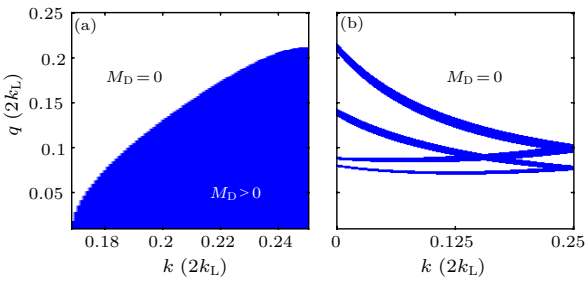

Fig. 5. (Color online) Dynamical stability phase diagrams for (a) period-doubled Bloch states of type I in the first band with $c = 0.4$; (b) period-doubled states of type I of the second band with $c = 4$. Here M_D denotes the maximum values among the imaginary part of eigenvalues of matrix $\sigma_z M_k(q)$; the blank areas are for $M_D = 0$. Here $V_0 = 0.1E_r$.

In our calculation we consider the states in Fig. 3. It is found that all period-doubled states of type Ⅱ (shown in Figs. 3(c) and 3(d)) have both Landau instability and dynamical instability. All the period-doubled Bloch states of type I shown in both Figs. 3(a) and 3(b) have Landau instability. The type-I states in the first band with higher nonlinear interaction c in Fig. 3(a) have dynamical instability. However, when c is small, for a given k there are always values of q where $M_D = 0$, corresponding to the blank areas shown in Fig. 5(a). There are also cases of $M_D = 0$ for type-I states in the second bands for different c as shown in Fig. 5(b). For the reflection symmetry of results in k and q, only the parameter region of $0 \le k \le 1/4$ and $0 \le q \le 1/4$ is shown. Nevertheless, as it is hard to control the modes of perturbations in actual experiments, from the point of experiments, these period-doubled states have dynamical instability.

In conclusion, we have systematically studied period-doubled Bloch states for a BEC in a one-dimensional optical lattice. Both our numerical and analytical results show that these period-doubled Bloch states can be viewed as growing out of seeds which are linear period-doubled states. We have found that all these period-doubled Bloch states suffer both Landau instability and dynamical instability. Some phenomena related period-doubled Bloch states have been observed experimentally.[22] However, it is still quite challenging to observe these states directly and clearly in a controlled way due to the fact that these period-doubled Bloch states are not stable. It would be interesting in the future to find stable period-doubled Bloch states by engineering the nonlinear interaction.

References

[1] Bloch I, Dalibard J and Zwerger W 2008 *Rev. Mod. Phys.* **80** 885
[2] Greiner M, Mandel M O, Esslinger T, Hänsch T and Bloch I 2002 *Nature* **415** 39
[3] Li B and Chen J B 2010 *Chin. Phys. Lett.* **27** 123701
[4] Wang X R, Yang Lu, Tan X Z, Xiong H W and Lü B L 2009 *Chin. Phys. Lett.* **26** 083701
[5] Zhu R 2007 *Chin. Phys. Lett.* **24** 797
[6] Zhu Q Z and Wu B 2015 *Chin. Phys.* B **24** 050507
[7] Qi W, Li Z H and Liang Z X 2018 *Chin. Phys. Lett.* **35** 010301
[8] Xu Z, Duan Y F, Zhou S Y, Hong T and Wang Y Z 2009 *Chin. Phys. Lett.* **26** 090303
[9] Jiang X, Lin M M, Li S C and Duan W S 2009 *Chin. Phys. Lett.* **26** 013701
[10] Diakonov D, Jensen L M, Pethick C J and Smith H 2002 *Phys. Rev.* A **66** 013604
[11] Machholm M, Pethick C J and Smith H 2003 *Phys. Rev.* A **67** 053613
[12] Wu B and Niu Q 2000 *Phys. Rev.* A **61** 023402
[13] Wu B, Diener R B and Niu Q 2002 *Phys. Rev.* A **65** 025601
[14] Wu B and Niu Q 2003 *New J. Phys.* **5** 104
[15] Chen Z and Wu B 2011 *Phys. Rev. Lett.* **107** 065301
[16] Mueller E J 2002 *Phys. Rev.* A **66** 063603
[17] Seaman B T, Carr L D and Holland M J 2005 *Phys. Rev.* A **72** 033602
[18] Wang D L, Yan X H and Wang F J 2007 *Chin. Phys. Lett.* **24** 1817
[19] Eiermann B, Anker Th, Albiez M, Taglieber M, Treutlein P, Marzlin K P and Oberthaler M K 2004 *Phys. Rev. Lett.* **92** 230401
[20] Zhang Y P, Liang Z X and Wu B 2009 *Phys. Rev.* A **80** 063815
[21] Machholm M, Nicolin A, Pethick C J and Smith H 2004 *Phys. Rev.* A **69** 043604
[22] Gemelke N, Sarajlic E, Bidel Y, Hong S and Chu S 2005 *Phys. Rev. Lett.* **95** 170404
[23] Gross E P 1963 *J. Math. Phys.* **4** 195
Pitaevskii L P 1961 *Zh. Eksp. Teor. Fiz.* **13** 451
[24] Görlitz A, Vogels J M, Leanhardt A E, Raman C, Gustavson T L, Abo-Shaeer J R, Chikkatur A P, Gupta S, Inouye S, Rosenb T and Ketterle W 2001 *Phys. Rev. Lett.* **87** 130402
[25] Cristiani M, Morsch O, Müller J H, Ciampini D and Arimondo E 2002 *Phys. Rev.* A **65** 063612
[26] Wu B and Niu Q 2001 *Phys. Rev.* A **64** 061603
[27] Cataliotti F S, Fallani L, Ferlaino F, Fort C, Maddaloni P and Inguscio M 2003 *New J. Phys.* **5** 71
[28] Fallani L, De Sarlo L, Lye J E, Modugno M, Saers R, Fort C and Inguscio M 2004 *Phys. Rev. Lett.* **93** 140406
[29] Sarlo L D, Fallani L, Lye J E, Modugno M, Saers R, Fort C and Inguscio M 2005 *Phys. Rev.* A **72** 013603
[30] Bronski J C, Carr L D, Deconinck B and Kutz J N 2001 *Phys. Rev. Lett.* **86** 1402
[31] Bronski J C, Carr L D, Deconinck B, Kutz J N and Promislow K 2001 *Phys. Rev.* E **63** 036612
[32] Smerzi A, Trombettoni A, Kevrekidis P G and Bishop A R 2002 *Phys. Rev. Lett.* **89** 170402

Chinese Physics Letters

Volume 35 Number 7 July 2018

CONDENSED MATTER: ELECTRONIC STRUCTURE, ELECTRICAL, MAGNETIC, AND OPTICAL PROPERTIES

CROSS-DISCIPLINARY PHYSICS AND RELATED AREAS OF SCIENCE AND TECHNOLOGY

GEOPHYSICS, ASTRONOMY, AND ASTROPHYSICS